

The variations of VOCs based on the policy change of Omicron in traffic-hub city Zhengzhou

Bowen Zhang^{1,3}, Dong Zhang^{2,3}, Zhe Dong^{2,3}, Xinshuai Song^{1,3}, Ruiqin Zhang^{1,3},
Xiao Li^{1,3,*}

¹School of Ecology and Environment, Zhengzhou University, Zhengzhou 450001,
China

²College of Chemistry, Zhengzhou University, Zhengzhou 450001, China

³Institute of Environmental Sciences, Zhengzhou University, Zhengzhou 450001,
China

Abstract: Online volatile organic compounds (VOCs) were monitored before and after the Omicron policy change at an urban site in polluted Zhengzhou from December 1, 2022, to January 31, 2023. The characteristics and sources of VOCs were investigated. The daily mean concentrations of PM_{2.5} and total VOCs (TVOCs) ranged from 53.5 to 239.4 $\mu\text{g}/\text{m}^3$ and 15.6 to 57.1 ppbv, respectively, with mean values of $111.5 \pm 45.1 \mu\text{g}/\text{m}^3$ and 36.1 ± 21.0 ppbv, respectively, throughout the period. Two severe pollution events (designated as Case 1 and Case 2) were identified in accordance with the National Ambient Air Quality Standards (NAAQS) (China's National Ambient Air Quality Standards (NAAQS) from 2012). Case 1 (December 5 to December 10, PM_{2.5} daily mean = $142.5 \mu\text{g}/\text{m}^3$) and Case 2 (January 1 to January 8, PM_{2.5} daily mean = $181.5 \mu\text{g}/\text{m}^3$) occurred during the infection period (when the policy of "full nucleic acid screening measures" was in effect) and the recovery period (after the policy was cancelled), respectively. The PM_{2.5} and TVOCs values for Case 2 are, respectively, 1.3 and 1.8 times higher than those for Case 1. The results of the positive matrix factor modeling demonstrated that the primary source of volatile organic compounds (VOCs) during the observation period was industrial emissions, which constituted 32% of the total VOCs, followed by vehicle emissions (27%) and combustion (21%). In Case 1, industrial emissions constituted the primary source of VOCs, accounting for 32% of the total VOCs. In contrast, in Case 2, the contribution of vehicular emission sources increased to 33% and became the primary source of VOCs. The secondary organic aerosol formation potential for Case 1 and Case 2 were found to be $37.6 \mu\text{g}/\text{m}^3$ and $65.6 \mu\text{g}/\text{m}^3$, respectively. In Case 1, the largest contribution of SOAP from industrial sources accounted for the majority (63%, $23.8 \mu\text{g}/\text{m}^3$), followed by vehicular sources (18%). After the end of the epidemic and the resumption of productive activities in the society,

34 the difference in the proportion of SOA generated from various sources decreased. Most
35 of the SOAP came from solvent use and fuel evaporation sources, accounting for 32%
36 (20.9 $\mu\text{g}/\text{m}^3$) and 26% (16.8 go/m^3), respectively. On days with minimal pollution,
37 industrial sources and solvent use remain the main contributors to SOA formation.
38 Therefore, regulation of emissions from industry, solvent-using industries and motor
39 vehicles need to be prioritized to control the $\text{PM}_{2.5}$ pollution problem.

40

41 **Keywords: Volatile organic compounds; Pollution episode; Source apportionment; Positive**
42 **Matrix Factorization model; Secondary organic aerosol formation potential;**

43 **1. Introduction**

44 Volatile organic compounds (VOCs) in the atmosphere have high reactivity and
45 can react with nitrogen oxides (NO_x) to form a series of secondary pollutants such as
46 ozone (O₃) and secondary organic aerosol (SOA), resulting in regional air pollution (Li
47 et al., 2019; Hui et al., 2020). The problem of O₃ pollution has been plaguing major
48 urban agglomerations in China (Zheng et al., 2010; Li et al., 2014; Wang et al., 2017).
49 SOA is an important component of fine particulate matter (PM_{2.5}) and contributes
50 significantly to haze pollution (Liu et al., 2019). PM_{2.5} remains the most significant air
51 pollutant in many Chinese cities for years (Shao et al., 2016; Wu et al., 2016). In
52 addition, VOCs, represented by the benzene homologues, can cause damage to kidneys,
53 liver, and nervous system of humans when they enter the body (Zhang et al., 2018).

54 Studies have shown that the most common VOC components in China are alkanes,
55 olefins, aromatic hydrocarbons, oxygenated VOCs (OVOCs), and halogenated
56 hydrocarbons, among which alkanes are the most abundant species (Liu et al., 2020;
57 Zhang et al., 2021a). VOCs in the atmosphere have a wide range of sources, and VOCs
58 in different regions are affected by multiple factors such as local geography, climate,
59 and human activities (Mu et al., 2023; Zou et al., 2023). The above reasons lead to
60 significant regional and seasonal differences in the characteristics of VOCs (Song et al.,
61 2021). For example, the annual average concentration of VOCs in the coastal
62 background area of the Pearl River Delta is 9.3 ppbv. The seasonal variation trend of
63 VOCs is high in autumn and winter and low in summer (Yun et al., 2021). In contrast,
64 the average VOC concentration in autumn and winter in Beijing was 22.6 ± 12.6 ppbv,
65 and the VOC concentration in the winter heating period was twice that in the autumn
66 non-heating period (Niu et al., 2022).

67 Moreover, the sources of VOC components in different regions are also related to
68 the local industrial structure and living habits. In rural areas of North China Plain in
69 winter, it is found that the SOA formation potential (SOAP) of VOCs under low NO_x
70 conditions is significantly higher than that under high NO_x conditions, and the increase
71 of aromatic hydrocarbon emissions caused by coal combustion is the main reason for
72 the higher SOAP in winter (Zhang et al., 2020). Li et al. (2022) found that the average
73 increased concentration of acetylene was 4.8 times from autumn to winter in the
74 Guanzhong Plain, indicating that fuel combustion during the heating period in winter
75 has a significant impact on the composition of VOCs. In contrast, continuous

76 observations conducted by Zhou et al. (2022) in the suburbs of Dongguan in summer
77 found that industrial solvent usage, liquefied petroleum gas (LPG) and oil and gas
78 volatilization were the main sources of VOCs. The results highlighted a wide variation
79 of characteristics, sources and chemical reactions of VOCs in the atmosphere thus it is
80 necessary to investigate VOCs in different cities when formulating control measures.

81 Zhengzhou, as the capital of Henan Province, is an important transportation hub
82 and economic center in the Central Plains region. Zhengzhou is currently facing
83 significant air pollution problems, with the Air Quality Index at the bottom of the
84 national ranking of 168 cities for many years. In January 2023, for example, the number
85 of polluted days with PM_{2.5} as the primary pollutant was 17, and the daily average value
86 of PM_{2.5} reached a maximum of 298 µg/m³
87 ([https://www.aqistudy.cn/historydata/daydata.php?city=%E9%83%91%E5%B7%9E](https://www.aqistudy.cn/historydata/daydata.php?city=%E9%83%91%E5%B7%9E&month=202301)
88 &month=202301, Accessed Jan 2024), which is almost 300% higher than the Chinese
89 daily average standard (grade II, 75 µg/m³). The studies of VOCs were carried out in
90 Zhengzhou in recent years, which focused on the characteristics and sources of VOCs
91 during pollution episodes (Lai et al., 2024) or before the coronavirus epidemic outbreak
92 (Li et al., 2020; Zhang et al., 2021b). While some atmospheric VOCs studies involving
93 the impact of Covid-19 lockdown have been performed in India (Singh et al., 2023a),
94 in China (e.g., Pei et al., 2022; Jensen et al., 2023; Zuo et al., 2024), or with respect to
95 toluene, benzene, m/p-xylene and ethylbenzene only (e.g., Sahu et al., 2022; Singh et
96 al., 2023b), a gap persisted in the investigation of VOCs due to the impact of
97 abolishment of China's zero-policy. Furthermore, some studies have discussed the
98 impact of changes in human production activities on air pollution during and after the
99 outbreak of the coronavirus disease (e.g., Ma et al., 2022; Jiang et al., 2023; Song et al.,
100 2023), but as mentioned earlier, only a few studies with in-depth exploration of the
101 changes in VOCs and none dealing with ending the zero-Covid policy during Omicron
102 variant infection period.

103 In this study, a continuous online observation of VOCs in polluted winter at an
104 urban site was carried out, which covered the abolishment of lockdown measures in
105 Zhengzhou. The focus of this study was on pollution events in which the daily average
106 PM_{2.5} concentration exceeded 75 µg/m³ (China's Class II standard) for more than three
107 consecutive days, and any day in which the PM_{2.5} concentration was less than 35 µg/m³
108 (China's Class I standard) was considered a clean day. China lifted the zero-COVID
109 strategies, notably by announcing the '10 measures' about the optimization of COVID-

110 19 rules on 7 December 2022 ([http://www.news.cn/politics/2022-](http://www.news.cn/politics/2022-12/07/c_1129189285.htm)
111 12/07/c_1129189285.htm, Accessed Jan 2024), which led to significant changes in
112 social activities. After that, China experiences a nationwide outbreak of COVID-19.
113 Our research primarily concentrates on the period dominated by COVID-19 Omicron
114 variant, where they demonstrate notable differences from the early virus strains (i.e.,
115 original SARS-CoV-2 virus and Delta) in terms of geographical transmission, the scale
116 of the infected population, and symptom manifestation (Petersen et al., 2022; Merino
117 et al., 2023). Zhengzhou Municipal Government in Henan Provincial People's
118 Government Portal (www.henan.gov.cn) on October 5, 2022 issued Circular No. 139,
119 the content of the circular is due to Zhengzhou during this period Omicron infection
120 cases frequently, in order to prevent the spread of the epidemic hidden, and therefore to
121 carry out the city's new coronavirus nucleic acid screening, screening scope for all
122 residents in the city area, at the same time, closed public places Suspension of business,
123 and to advise residents to reduce activities outside, and the content of the above notice
124 similar to the notice continued to be issued until the Circular No. 162. The epidemic
125 prevention and control measures in Zhengzhou changed to tin Circular No. 163 issued
126 on December 4, 2022, restoring the opening of closed public places; Circular No. 164
127 issued on December 8 announced that it was no longer necessary to present health codes
128 and nucleic acid negative certificates for the movement of people, and that centralized
129 isolation would no longer be adopted for those who were positive for the infection.
130 Since then, the number of people moving around Zhengzhou has increased and social
131 production has resumed.

132 After the quarantine policy was lifted, people basically rested at home due to
133 infection or fear of infection with Omicron. The resumption of normal production and
134 life depends on herd immunization. This outbreak event is the longest in duration and
135 the largest in number of infections since the 2020 outbreak of the novel coronavirus in
136 Zhengzhou. It would be beneficial to investigate the impact of this event on emissions
137 related to transportation and industrial production. This change is worth exploring in
138 terms of its impact on transportation and industrial production emissions. Therefore,
139 the characteristics and variations of VOCs during different periods were investigated to
140 assess their impact on the formation of SOA and to provide data support for future
141 pollution control policies in Zhengzhou.

142

143 **2. Materials and methods**

144 **2.1 Sample collection and Chemical analysis**

145 The online VOCs observation station is located on the roof of the Zhengzhou
146 Environmental Protection Monitoring Center, which is in the urban area. The sampling
147 site is close to main roads on three sides (150 m away from Funiu Road on the east side,
148 200 m away from Qinling Road on the west side, and connected to Zhongyuan Road
149 on the south side), and surrounded by residential areas and commercial areas without
150 other large nearby stationary sources. The sampling period for this study was from
151 December 1, 2022, to January 31, 2023, which is always the most polluted period in
152 the entire year. Apart from a brief occurrence of rain and snow on December 25, the
153 sampling days were either sunny or cloudy. The wind speed (WS), temperature (Temp)
154 and relative humidity (RH) during this period were 1.3 ± 0.9 m/s, 5.3 ± 3.2 °C and 38.9
155 $\pm 19.0\%$), respectively, similar to the values observed in previous years in Zhengzhou.
156 It is interesting to point out that the sampling period in the present study covered the
157 entire infection period of Omicron in Zhengzhou, including the phase of surge in
158 infected population (Infection period, from 2022.12.01 to 2022.12.31) and restoration
159 of production and livelihood phase (Recovery period, from 2023.1.1 to 2023.1.31 in
160 2023) (Fig. S1, Chinese Center for Disease Control and Prevention, 2023).

161 The VOCs were measured hourly using a GC-FID/MS (TH-PKU 300 b, Wuhan
162 Tianhong Instruments Co., China). The instrument TH-PKU300b includes electronic
163 refrigeration ultra-low temperature pre-concentration sampling system, analysis system
164 and system control software. The ambient VOCs in the first 5 minutes of each hour
165 were collected by the sampling system and then entered the concentration system.
166 Under low temperature conditions, the VOCs samples collected were frozen in the
167 capillary capture column, and then quickly heated and resolved, so that the compounds
168 entered the analysis system. After separation by chromatographic column, the
169 compounds were monitored by FID and MS detectors. During the detection process,
170 the atmospheric samples collected undergo analysis through two distinct pathways. C2-
171 C5 hydrocarbons are analyzed using FID, while C5-C12 hydrocarbons, halocarbons,
172 and OVOCs are analyzed with a MS detector. After excluding species with missing data
173 exceeding 10%, the detected volatile organic compounds include 29 alkanes, 11 alkenes,
174 17 aromatics, 35 halocarbons, 12 OVOCs, 1 alkyne (acetylene), and 1 sulfide (CS₂)
175 with a total of 106 compounds. A detailed description of the instrumentation can be

176 found in our previous study (Zhang et al., 2021; Shi et al., 2024; Zhang et al., 2024).

177 The instrument was calibrated per week to ensure the accuracy of VOCs by
178 injecting standard gases with a five-point calibration curve. The detection limit of C2-
179 C5 hydrocarbons ranges from 0.007 to 0.099 ppbv, other hydrocarbons are 0.004–0.045
180 ppbv, halogenated hydrocarbons 0.009-0.099 ppbv, OVOCs and other compounds of
181 0.006–0.095 ppbv. Thirty-two of the monitored VOCs had over 90% observed data
182 greater than the detection limit, and 34 had more than 50% observed data greater than
183 the detection limit.

184 Simultaneous observations at the same site were also carried out for particulate
185 matter (PM_{2.5}, PM₁₀), other trace gases (carbon monoxide (CO), O₃, nitric oxide (NO),
186 nitrogen dioxide (NO₂)), and meteorological data (Temperature, RH, WS, and wind
187 direction (WD)) based on 1 h resolution.

188 2.2 Positive Matrix Factorization (PMF) model

189 EPA PMF5.0 model was used for the quantitative source analysis of VOCs (Norris
190 et al., 2014). The principles and methods have been described in detail in previous
191 studies (Mozaffar et al., 2020; Zhang et al., 2021b). The decomposition of the PMF
192 mass balance equations is simplified as follows (Norris et al., 2014):

193

$$194 \quad x_{ij} = \sum_{k=1}^p g_{ik} f_{kj} + e_{ij} \quad (1)$$

195

196 where x_{ij} is the mass concentration of species j measured in sample i ; g_{ik} is the
197 contribution of factor k to the sample i ; f_{kj} represents the content of the j th species in
198 factor k ; e_{ij} is the residual of species j in sample i ; p represents the number of factors.
199 The fitting objective of the PMF model is to minimize the function Q to obtain the
200 factor contributions and contours. The formula for Q is given in Eq. (2):

201

$$202 \quad Q = \sum_{i=1}^n \sum_{j=1}^m \left[\frac{x_{ij} - \sum_{k=1}^p g_{ik} f_{kj}}{u_{ij}} \right]^2 \quad (2)$$

203

204 where n and m denote the number of samples and VOC species, respectively.

205 Concentrations and uncertainty data are required for the PMF model. In this study,
206 the median concentration of a given species is used to replace missing values with an
207 uncertainty of four times of the median values; data less than the Method Detection
208 Limit (MDL) were replaced with half the MDL, with an uncertainty of 5/6 of the MDL;
209 and the uncertainty for values greater than the MDL was calculated using Eq. (3). In
210 Eq. (3), EF is error fraction, expressed as the precision of VOCs species, and the setting
211 range can be adjusted from 5 to 20% according to the concentration difference (Buzcu
212 et al., 2006; Song et al., 2007); and c_{ij} is the concentration of species j in sample i :

$$213 \quad U_{ij} = \sqrt{(EF \times c_{ij})^2 + (0.5 \times MDL)^2} \quad (3)$$

214 when the concentration of VOCs in the species is less than the value of the
215 detection limit U_{ij} is calculated using Eq. (4):

$$216 \quad U_{ij} = \left(\frac{5}{6}\right) MDL \quad (4)$$

217 VOC species and concentration input into PMF were carefully selected to ensure
218 the accuracy of the PMF results. Species were excluded when over 25% of the samples
219 were missing or concentrations values were below the MDL (Gao et al., 2018); VOCs
220 with a short lifetime in the atmosphere were also excluded unless they are source-
221 relative species (Zhang et al., 2014; Shao et al., 2016). After that, retained VOC species
222 were categorized according to the signal-to-noise ratio (S/N) with $S/N < 0.2$ species
223 categorized as bad, $0.2 < S/N < 2$ species categorized as weak; and $S/N > 2$ species
224 categorized as strong (Shao et al., 2016).

225 We used displacement of factor elements (DISP) to assess PMF modelling
226 uncertainty (for a description, see Paatero et al. (2014)). Q was less than 1% and no
227 swaps occurred for the small est dQ^{\max} in DISP. F_{peak} values from -2 to 2 were tested
228 to explore the rotational stability of the solutions. $Q_{\text{true}}/Q_{\text{exp}}$ is lowest when $F_{\text{peak}} = 0$,
229 so we chose the PMF results for that case (Fig. S2a). After examining 3-8 factors, 20
230 base runs with 5 factors eventually selected to represent final result. We provide an
231 explanation of factor selection in the supplementary materials. Fig. S2(b) includes
232 $Q_{\text{true}}/Q_{\text{exp}}$, $Q_{\text{robust}}/Q_{\text{exp}}$ for factors 3-8. The slopes of these two ratios in changed at five
233 factors, and we found that five factors were more realistic after repeated comparisons
234 of the results at four, five and six factors.

235 **2.3 SOA generation potential**

236 The contributions of VOC species to SOAP were calculated based on the toluene
237 weighted mass contributions (TMC) method (Derwent et al., 2010). The methodology
238 for calculating SOAP is as follows:

$$239 \text{SOAPF}_i = \frac{\text{VOCs component } i \text{ to SOA mass concentration increments}}{\text{Toluene to SOA mass concentration increment}} \times 100 \quad (5)$$

241
242 SOAPF_i for each VOC is taken from the literature (Derwent et al., 2010). The
243 SOAP was estimated by multiplying the SOAPF_i value by the concentration of
244 individual VOC species. The SOAP calculations through each VOC are as follows:

$$245 \text{SOAP} = \sum E_i \times \text{SOAPF}_i \quad (6)$$

246 E_i is the concentration of species i .

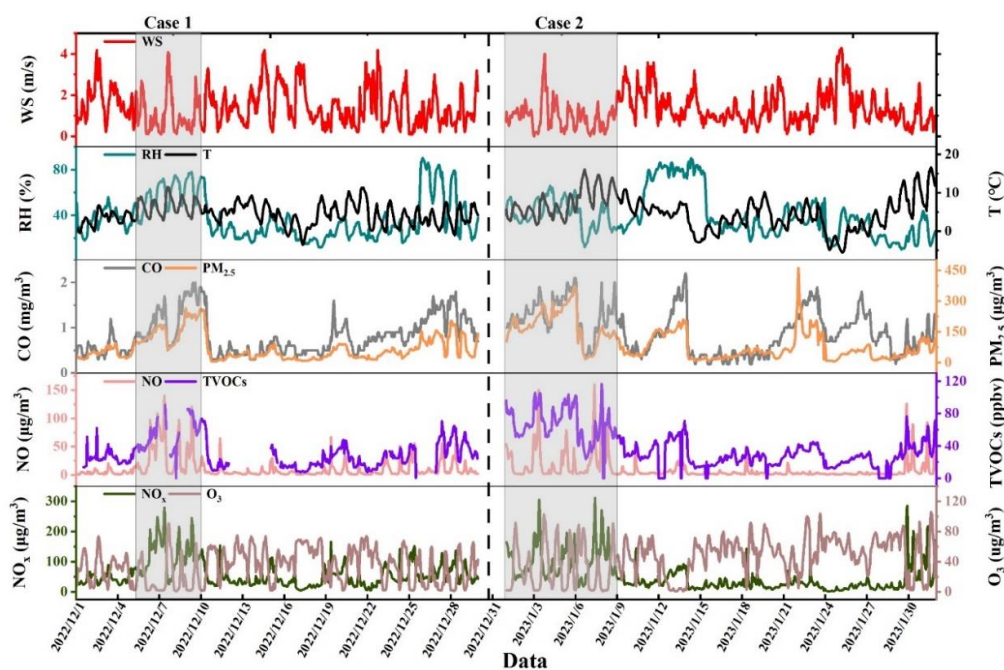
249 **3. Results and discussion**

250 **3.1 Overview of variation in pollutants and meteorological** 251 **parameters**

252 Figure 1 shows the time series of meteorological parameters, TVOCs, O₃, NO_x,
253 SO₂, CO and PM_{2.5} during the observed periods. Low WS and Temperature were found
254 with an average value of 1.3 ± 0.6 m/s and 5.0 ± 2.5 °C, respectively, during the entire
255 period, comparable with observations at the same site in 2021 (Lai et al., 2024). A total
256 of 62 days of valid data was acquired with the daily average concentration of PM_{2.5}
257 ranging from 53 to 239 $\mu\text{g}/\text{m}^3$, with the average value of 111 ± 45 $\mu\text{g}/\text{m}^3$. The
258 concentration of TVOCs ranged from 15.6 to 57.1 ppbv with an average of 36.1 ± 21.0
259 ppbv, higher than the same period in last year (27.9 ± 12.7 ppbv, Lai et al., 2024).
260 During the observation period, the average values of T, WS and RH were 5.0 ± 2.5 °C,
261 1.3 ± 0.6 m/s and $38.9 \pm 16.7\%$, respectively.

262 Previous studies have shown that meteorological factors such as low wind speed,
263 high relative humidity, and low precipitation are responsible for the increase in
264 particulate matter pollution in Zhengzhou in winter (Duan et al., 2019). Our analysis
265 of the correlation between different pollutants and meteorological conditions during

266 the pollution period showed that PM_{2.5}, TVOCs and NO_x were positively correlated
 267 with relative humidity (Fig. S3), which is consistent with the results of some previous
 268 studies (Wang et al., 2019). The comparisons of average concentrations of different
 269 periods between different periods are presented in Tables 1 and 2. The comparison
 270 between polluted and clean days shows that the wind speed is lower than that of clean
 271 days and the humidity is higher than that of clean days, which is consistent with the
 272 meteorological conditions characterized by the occurrence of polluted days. WS,
 273 Temp and RH conditions during infection and recovery periods were generally similar.
 274 However, the average concentration of PM_{2.5} during the recovery period was 1.6 times
 275 the value during the infection period. Furthermore, the concentrations of other
 276 pollutants including SO₂, NO₂, CO, and O₃ all showed a similar trend between
 277 infection and recovery periods. The TVOCs concentration during the recovery period
 278 was 1.2 times the value during the infection period, showing an obvious increase trend
 279 after resuming production. A comparison of the meteorological conditions associated
 280 with the two pollution processes revealed no discernible trend towards greater
 281 susceptibility to pollution. However, the concentrations of pollutants in Case 2 were
 282 significantly higher than in Case 1, a trend that is most likely attributable to the
 283 resumption of production activities and increased emissions during Case 2. Decreased
 284 trends of air pollutants were found in other studies before and after the outbreak of the
 285 novel coronavirus (COVID-19) in early 2020 (Qi et al., 2021; Wang et al., 2021).



286
 287

Fig. 1. Time series of WS, T, RH, CO, PM_{2.5}, NO, TVOCs, NO_x and O₃ during the observation

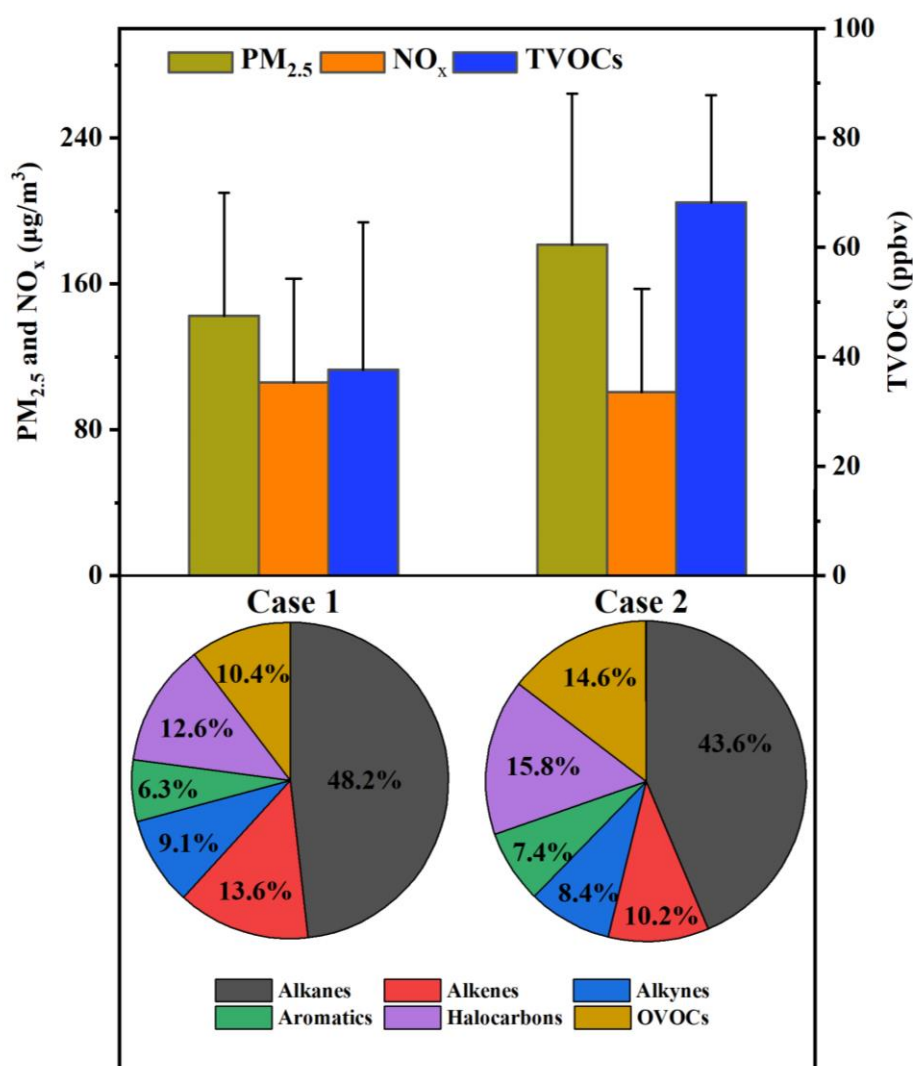
288

period.

289

The shadow section in Fig. 1 represents two haze pollution events during the monitoring period. A pollution event is determined when the daily average concentration of PM_{2.5} exceeds 75 μg/m³ (China's II-level standard) for at least three consecutive days. Case 1 (December 5 to December 10 with daily average PM_{2.5} = 142.5 μg/m³) and Case 2 (January 1 to January 8 with daily average PM_{2.5} = 181.5 μg/m³) were selected as they represent the pollution events in infection and recovery periods, respectively, due to their long duration and high pollution levels. Any day with a PM_{2.5} concentration lower than 35 μg/m³ (China's I-level standard) is considered as Clean days.

297



298

299

Fig. 2. The concentration of PM_{2.5}, NO_x, TVOCs and the composition ratio of VOCs in Case 1 and Case 2.

300

301

As for the two representative pollution processes (Case 1 during the infection period and Case 2 during the recovery period), the concentration of TVOCs in Case 1

302

303 and Case 2 were 48.4 ± 20.4 and 67.6 ± 19.6 ppbv (Fig. 2), respectively, increased by
 304 63% and 188% compared with values during clean days. The average concentrations
 305 of $PM_{2.5}$ and TVOCs during Case 2 were 1.3 and 1.8 times the values in Case 1. The
 306 highest volume contributions of alkanes were found both in Case 1 (48%) and Case 2
 307 (44%), consistent with the results in the Yangtze River Delta region (36-43%, Liu et al.,
 308 2023). While alkenes exhibited higher volume percentages of 13% in Case 1, followed
 309 by halogenated hydrocarbon (12%) and OVOCs (10%). Higher volume percentages of
 310 alkanes and alkenes in Case 1 were similar to the results in the gasoline evaporation
 311 site in winter (Niu et al., 2022). Equivalent volume contribution of halogenated
 312 hydrocarbon and OVOCs (15%) were found in Case 2, followed by alkenes (10%).
 313 **Although aromatic hydrocarbons have the lowest volumetric contribution (6% in Case**
 314 **1 and 7% in Case 2), they show the largest increase from clean days to pollution.**

315 Table 1 The average concentrations of meteorological parameters and pollutants during different
 316 processes.

Category	Entire process (2022.12.1- 2023.1.31)	Infection period (2022.12.1- 2022.12.31)	Recovery period (2023.1.1- 2023.1.31)	Case 1 (2022.12.5- 2022.12.10)	Case 2 (2023.1.1- 2023.1.10)	Clean Days
	N = 62 days	N = 31 days	N = 31 days	N = 6 days	N = 8 days	N = 8 days
WS (m/s)	1.3 ± 0.6	1.4 ± 0.6	1.3 ± 0.6	1.2 ± 0.9	0.9 ± 0.7	1.4 ± 0.8
T (°C)	5.0 ± 2.5	4.7 ± 1.7	5.4 ± 3.1	6.1 ± 2.2	7.4 ± 3.5	4.1 ± 3.0
RH (%)	38.9 ± 16.7	37.6 ± 15.5	40.2 ± 18.2	55.7 ± 14.7	42.0 ± 12.1	29.5 ± 18.1
TVOCs (ppbv)	36.1 ± 21.0	31.9 ± 18.1	39.8 ± 22.4	37.6 ± 27.0	68.2 ± 19.6	22.7 ± 11.1
SO ₂ (µg/m ³)	11.4 ± 2.7	10.2 ± 2.8	12.7 ± 2.3	11.0 ± 3.7	16.2 ± 6.1	6.5 ± 2.5
NO ₂ (µg/m ³)	47.2 ± 10.0	46.8 ± 8.6	47.8 ± 11.7	62.7 ± 20.5	65.0 ± 21.3	20.8 ± 15.9
CO (mg/m ³)	0.9 ± 0.2	0.8 ± 0.2	1.1 ± 0.2	1.2 ± 0.5	1.3 ± 0.4	0.5 ± 0.2
O ₃ (µg/m ³)	34.9 ± 6.0	31.1 ± 4.5	39.0 ± 4.6	21.8 ± 23.7	32.5 ± 29.6	52.6 ± 18.4
PM _{2.5} (µg/m ³)	111.5 ± 45.1	86.6 ± 34.6	138.3 ± 39.6	142.5 ± 67.4	181.5 ± 82.7	23.8 ± 16.8

317 Table 2 Concentration of VOC species during different processes (ppbv).

Category	Entire process	Infection period	Recovery period	Case 1	Case 2	Clean days
TVOCs	36.1 ± 21.0	31.9 ± 18.1	39.8 ± 22.4	48.4 ± 20.4	67.6 ± 19.6	17.5 ± 9.5
alkanes	16.8 ± 9.2	15.0 ± 8.4	18.4 ± 9.5	23.1 ± 10.0	29.5 ± 8.4	9.2 ± 5.6
alkenes	4.1 ± 2.7	3.8 ± 2.6	4.4 ± 2.7	6.5 ± 2.9	7.0 ± 2.6	1.7 ± 1.3
alkynes	3.1 ± 2.0	2.7 ± 1.7	3.4 ± 2.1	4.3 ± 2.0	5.8 ± 1.9	1.3 ± 0.8
aromatics	2.1 ± 2.0	1.8 ± 1.5	2.3 ± 2.2	3.0 ± 1.8	4.9 ± 2.8	0.7 ± 0.5

halogenated hydrocarbon	5.4 ± 3.3	4.4 ± 2.3	6.2 ± 3.8	6.0 ± 1.9	10.7 ± 3.6	2.7 ± 1.4
OVOcs	4.6 ± 3.2	3.5 ± 2.7	5.1 ± 3.5	5.0 ± 2.4	9.7 ± 2.8	1.9 ± 1.1

318 3.2 Source Analysis of VOCs

319 Specific VOC ratios can be used for initial source identification of VOCs and
 320 determination of photochemical ages of air masses (Monod et al., 2001; An et al., 2014;
 321 Li et al., 2019). In this study, the ratios of toluene/benzene (T/B), isopentane/n-pentane,
 322 isobutane/n-butane, and m/p-xylene/ethylbenzene (X/E) were selected to initially
 323 identify the potential sources of VOCs (Fig. 3). Concentrations of selected pollutants
 324 and ratios used are shown in Table S1.

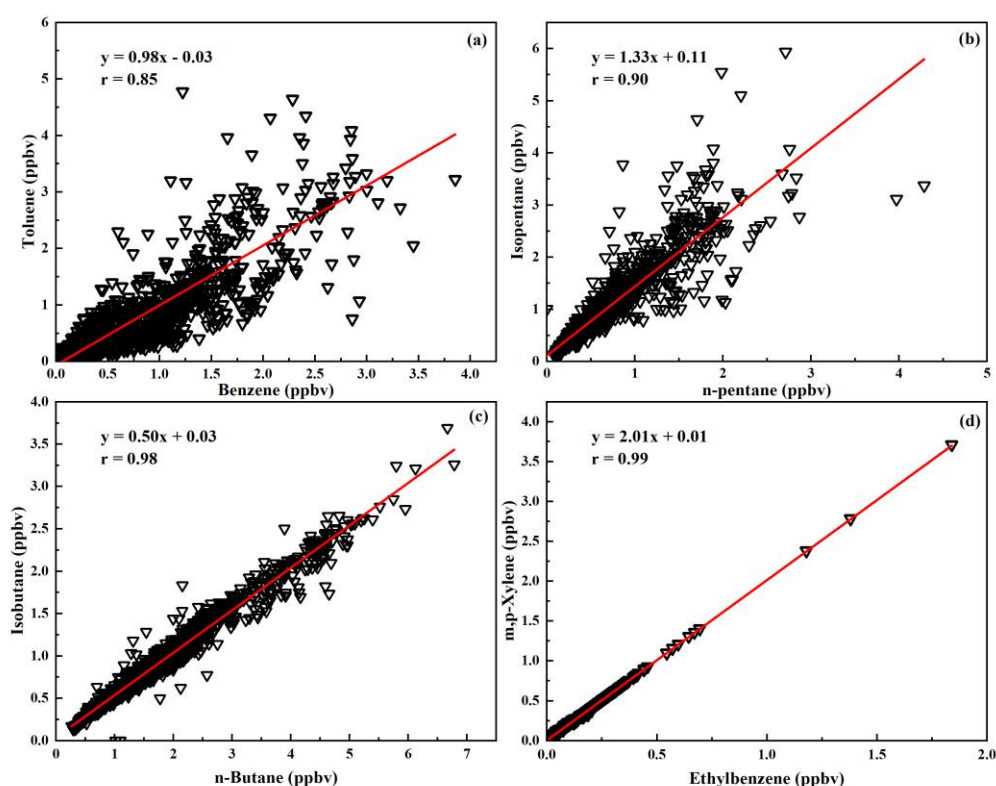
325 Toluene-to-benzene ratio (T/B ratio) was widely used to assess the relative
 326 importance of different sources. Specifically, T/B ratio with the value of 1.3–3.0 was
 327 observed in vehicle emissions for vehicles with different fuel types (Schauer et al., 2002;
 328 Wang et al., 2015). The reported T/B ratio for combustion processes was between 0.13
 329 and 0.7 (Li et al., 2011; Wang et al., 2014). The average T/B value for the entire period
 330 was 1.0, indicating that both traffic emissions and combustion are significant sources
 331 of VOCs.

332 The isopentane/n-pentane concentration ratios of 0.6-0.8 represent mainly coal
 333 combustion emissions, ratios of 0.8-0.9 represent liquefied petroleum gas (LPG)
 334 emissions, 2.2-3.8 represent vehicle exhaust emissions, and 1.8-4.6 represent fuel
 335 evaporation (Conner et al., 1995; Liu et al., 2008; Li et al., 2019). The overall ratio of
 336 isopentane/n-pentane is 1.4, indicating that pentane is mainly derived from the
 337 combined effects of liquid petrol and fuel evaporation.

338 Isobutane/n-butane concentration ratios of 0.2-0.3 represent vehicle emissions,
 339 0.4-0.6 represent LPG usage, and 0.6-1.0 represent natural gas emissions (Russo et al.,
 340 2010; Zheng et al., 2018). The ratio of isobutane/n-butane in this study was 0.50, which
 341 suggests that the VOC concentrations at the observation sites are influenced by natural
 342 gas emissions (Shao et al., 2016; Zeng et al., 2023).

343 The ratio of X/E can be used to infer the photochemical age of the air mass. X/E
 344 ratios around 2.5-2.9 are typical of urban areas, indicating that VOCs are mainly from
 345 the urban area (fresh air mass) (Kumar et al., 2018). When this ratio is significantly
 346 lower than 3, it indicates that VOCs are mainly transported from distant sources (aging
 347 air masses) (Kumar et al., 2018). The average X/E value in this study was 2.0 (Fig.
 348 3(d)), indicating low photochemical activity and aging of the air mass at the observation

349 site. Potential source analyses also indicate that air masses are affected by long-range
350 transport (Fig. S4).



351

352 Fig. 3. Correlation analysis between specific VOC species.

353 Figure 4 shows the chemical profiles of individual VOCs resolved by the PMF
354 model during the entire observation period. These five factors eventually selected as
355 potential sources for the observed VOCs are: (1) Fuel evaporation; (2) Solvent usage;
356 (3) Vehicular emission; (4) Industrial source; and (5) Combustion. These 5 factors have
357 been commonly reported before, e.g., in Shijiazhuang, northern China (Guan et al, 2023)
358 and in Beijing (Cui et al., 2022).

359 Alkanes of C4-C6 substances were predominant in factor 1, including 2-
360 methylpentane, 3-methylpentane, isobutane, n-butane, isopentane and n-pentane from
361 oil and gas (Xiong et al., 2020). Fig. S5 shows that emissions from this source peak at
362 midday, when fuel volatilization is high, The CPF plot shows that south-east is the
363 dominant direction at wind speeds of less than 2 m/s (Fig. 5a). Therefore, factor 1 was
364 identified as the source of oil and gas volatilization.

365 The contribution of benzene, toluene, methylene chloride, 1,2-dichloroethane and
366 ethyl acetate was high in factor 2. It has been shown that benzene, toluene, ethylbenzene,

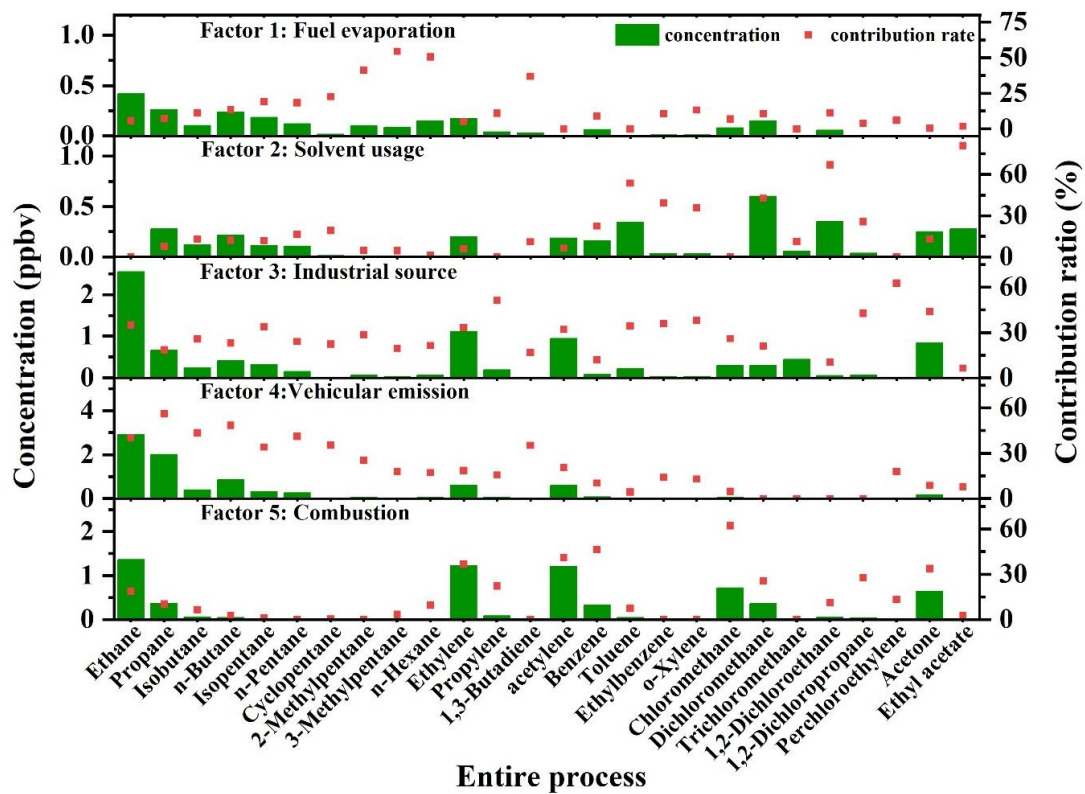
367 and xylene is an important component in the use of solvents (Li et al., 2015); methylene
368 chloride is often used as a chemical solvent, while esters are mostly used as industrial
369 solvents or adhesives (Li et al., 2015). Factor 2 is determined to be solvent usage source.

370 The CPF plot shows that due east is the main emission direction at wind speeds less
371 than 2 m/s and southeast is the main source at wind speeds greater than 2 m/s (Fig. 5b).

372 Factor 3 contains predominantly C3-C8 alkanes, olefins and alkynes, and
373 relatively high concentrations of benzene. These substances are usually emitted by
374 industrial processes (Shao et al., 2016), so Factor 4 is defined as an industrial source.
375 The CPF plots indicate that a local source at low wind speeds is the dominant sources
376 (Fig. 5c).

377 Factor 4 is characterized by relatively high levels of C2-C6 low-carbon alkanes
378 (ethane, propane, isopentane, n-pentane, isobutane and n-butane), olefins (ethylene and
379 propylene), and benzene and toluene, which are important automotive exhaust tracers
380 (Song et al., 2021; Zhang et al., 2021b). Ethylene and propylene are important
381 components derived from vehicle-related activities. Previous studies of VOCs in
382 Zhengzhou have shown a high percentage of VOCs emitted from gasoline vehicles,
383 with the main source of alkanes being on-road mobile sources (Bai et al., 2020). The
384 daily variation of this source in Fig. S5 shows a bimodal trend, with peaks occurring in
385 the morning and evening peaks of traffic, consistent with motor vehicle emissions. Fig.
386 5d shows that this source is mainly from the west where wind speeds are below 2 m/s,
387 and in this direction, there are a number of urban arterial roads with high traffic volumes.
388 Therefore, factor 4 was defined as vehicular emission source.

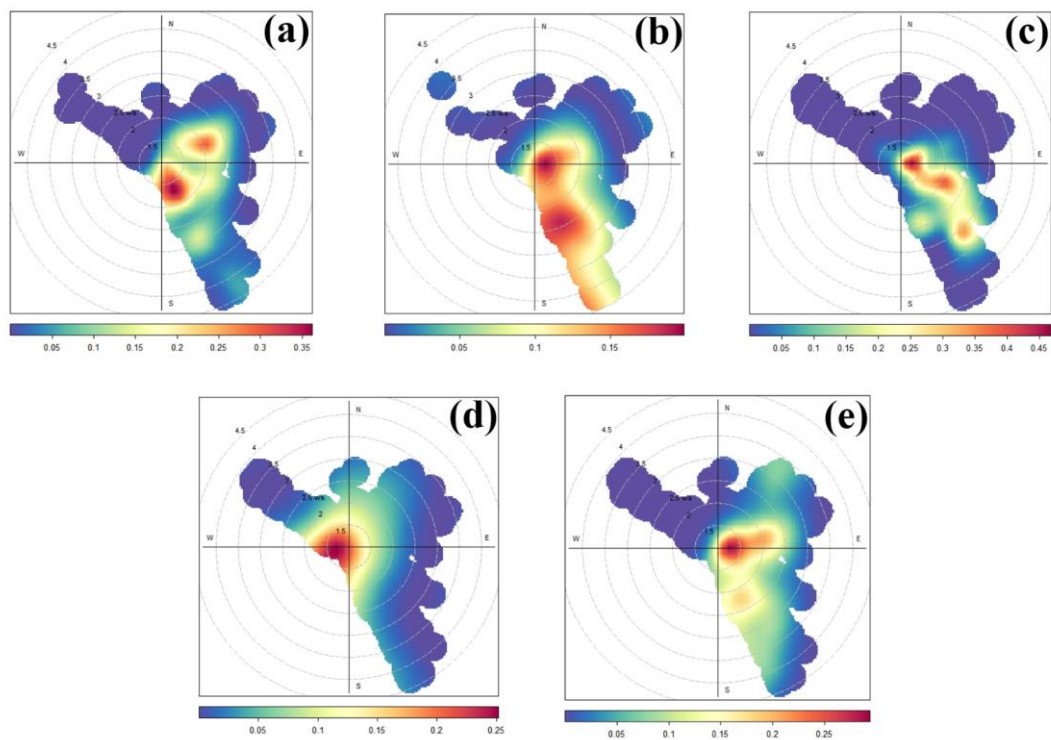
389 The highest contribution to factor 5 is chloromethane (62%). Benzene (46%) and
390 acetylene (41%) also contribute highly to factor 5. Chloromethane is the key tracer for
391 biomass combustion and acetylene is the key tracer for coal combustion (Xiong et al.,
392 2020). Therefore, factor 5 is defined as a combustion source. The CPF plot shows that
393 at wind speeds below 2 m/s, the north-east direction is the dominant source direction
394 (Fig. 5e).



395

396

Fig. 4. Concentration of VOC species in each factor and contribution to each source.



397

398

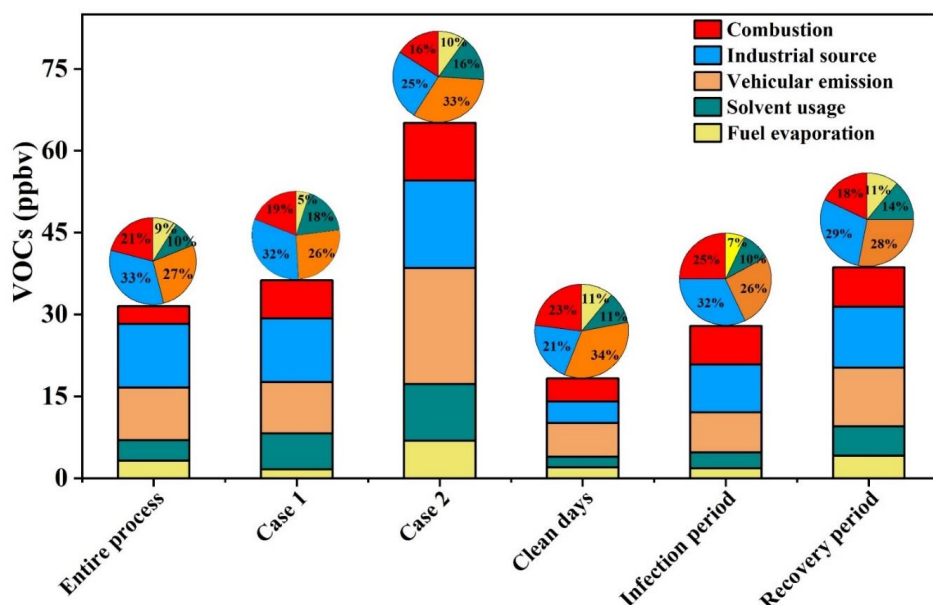
Fig. 5. CPF plots of five VOCs sources obtained using the PMF model.

399
400

Note: a: Fuel evaporation; b: Solvent usage; c: Industrial source; d: Vehicular emission; e:
Combustion.

401 Fig. S6 compares the differences in PMF source profiles between the Omicron
402 infection period and the recovery period, as well as between the pollution day and the
403 clean day. We present the concentrations of the five main VOCs in all five factors in
404 Table S2. Ethane (vehicular emission), 2-methylpentane (fuel evaporation), benzene
405 (industry source), chloromethane (combustion), and ethyl acetate (solvent usage) were
406 selected as tracers for five sources. Ethane concentration in Case 2 (5.9 ppbv) is much
407 higher than in other processes, and ethane concentration during the recovery period (3.4
408 ppbv) is also higher than during the infection period (2.4 ppbv), which may to some
409 extent reflect increased vehicular emissions during the recovery period.

410 Concentrations of most species were significantly higher during the recovery
411 period than during the infection period. The representative pollution processes in both
412 periods showed the same results as well, with a 79% higher concentration of TVOCs in
413 Case 2 (65.1 ppbv) compared to Case 1 (36.3 ppbv) (Fig. 6). While in Case 1 industry
414 was the dominant source of VOCs, by Case 2 motorized sources reached a
415 concentration value of 21.2 ppbv, accounting for 33% of the observed VOCs, and
416 became the dominant source of emissions. This is consistent with the fact that people's
417 mobility activities have increased after the epidemic has entered the recovery period.
418 As a group of VOCs species with the highest concentration share, ethane and propane
419 contributed more to the clean days motor vehicle source than other processes, which
420 also resulted in a 34% clean days motor vehicle source share.

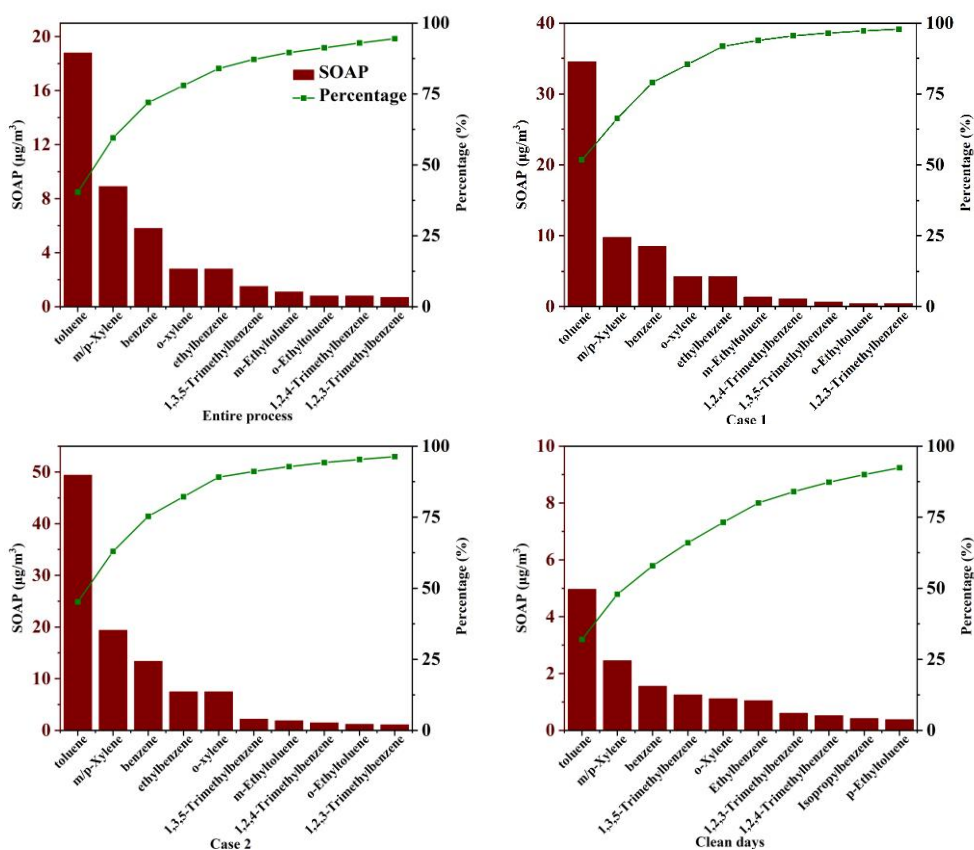


421

423 **3.3 SOAP**

424 VOCs are estimated to contribute about 16–30% or more of PM_{2.5} by mass through
 425 SOA production (Huang et al., 2014). Therefore, by calculating the SOAP value, the
 426 influence of different sources on PM_{2.5} production can be reflected to a certain extent.

427 We have included quantitative analysis for SOAP as well. Fig. 7 shows the SOAP
 428 concentrations and contribution rates of the top ten species throughout the entire
 429 process, during two pollution processes, and clean days. The top ten species all reached
 430 close to 100% of the total SOAP contribution, with Case 1 reaching 98%. In each
 431 process, the composition of the top ten substances is essentially the same. Aromatic
 432 hydrocarbons contributed the most, with BTEX always occupying the top five positions
 433 and toluene the most. The SOAP values of the top ten contributing species for the two
 434 polluting processes are shown in Tables S3 and S4. Toluene, the highest contributing
 435 species, reached a SOAP value of 49.4 $\mu\text{g}/\text{m}^3$ in the most polluted Case 2, which was
 436 3.2 times higher than the SOAP sum of all species on the clean day (15.5 $\mu\text{g}/\text{m}^3$). The
 437 SOAP value for Case 1, which is also a contaminated process, was 67 $\mu\text{g}/\text{m}^3$, and the
 438 main species (m/xylylene: 9.8 $\mu\text{g}/\text{m}^3$, benzene: 8.5 $\mu\text{g}/\text{m}^3$) including toluene (34.6 $\mu\text{g}/\text{m}^3$)
 439 were lower than those for Case 2 (m/xylylene: 19.4 $\mu\text{g}/\text{m}^3$, benzene: 13.4 $\mu\text{g}/\text{m}^3$).

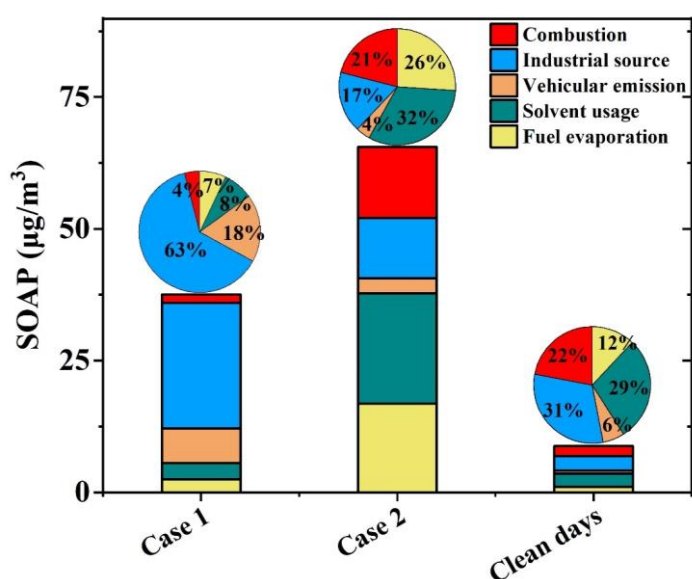


441

Fig. 7. SOAP dominant species in different processes

442

443 Figure 8 shows the SOAP calculated after source resolution of the two pollution
444 processes by PMF for clean days, respectively. In Case 1, industrial source is the
445 dominant source with a contribution ratio of 63%. In Case 2, the pollution sources
446 exhibit a more evenly distributed contribution, where the solvent usage and fuel
447 evaporation sources emerge as the primary contributors to SOAP, with their respective
448 contribution levels rising to 32% and 26%. Case 1 was during the infection period,
449 when social activities had not yet returned to normal. In Case 2, when society had
450 basically returned to normal, the increase in emissions from various sources resulted in
451 a more balanced distribution of SOAP contributions and caused more severe PM_{2.5}
452 pollution. In addition, a few days before Case 2, the Zhengzhou Municipal People's
453 Government initiated the Heavy Pollution Weather Level II response
454 (<https://sthjj.zhengzhou.gov.cn/tzgg/7037130.jhtml>) and introduced control measures
455 for emissions from industrial and mobile sources, which resulted in a significant
456 reduction of SOAP levels from industrial and motorized sources in Case 2. The clean
457 day result with a SOAP of 8.8 µg/m³ also indicates that industrial and solvent usage
458 sources are the most dominant SOAP sources. The primary sources of aromatic
459 compounds, which are the most significant contributors to SOAP, are solvent usage and
460 industrial process emissions. This finding aligns with the results of other studies (Wu
461 et al., 2017). Consequently, it is imperative to implement measures to reduce PM_{2.5}
462 pollution by regulating emissions from industrial and solvent usage sources.



462

463

Fig. 8. SOAP value and contribution ratio of each process

464

465 4. Conclusions

466 Continuous observation of VOCs during the infection of the Omicron epidemic
467 was carried out at an urban site in polluted Zhengzhou from December 1, 2022, to
468 January 31, 2023. The daily average concentration of PM_{2.5} ranged from 53.5 to 239.4
469 $\mu\text{g}/\text{m}^3$ with an average value of $111.5 \pm 45.1 \mu\text{g}/\text{m}^3$ during the whole period. The
470 concentration of TVOCs ranged from 15.6 to 57.1 ppbv with an average of 36.1 ± 21.0
471 ppbv, higher than the same period in last year (27.9 ± 12.7 ppbv, Lai et al., 2024). Two
472 representative contamination processes were identified (Case 1 during the infection
473 period and Case 2 during the recovery period). The concentration of TVOCs in Case 1
474 and Case 2 were 48.4 ± 20.4 and 67.6 ± 19.6 ppbv, respectively, increased by 63% and
475 188% compared with values during clean days. The average concentrations of PM_{2.5}
476 and TVOCs during Case 2 were 1.3 and 1.8 times of the values in Case 1. This is
477 consistent with the observed increase in pollutant emissions following the return to
478 normal social life from the period of Omicron infection. The highest volume
479 contributions of alkanes were found both in Case 1 (48%) and Case 2 (44%). Though
480 the volume contribution of aromatics were the lowest (6% in Case 1 and 7% in Case 2),
481 the highest increase ratio was found from clean days to polluted episodes. Low wind
482 speed and high humidity were the main meteorological reasons for the occurrence of
483 pollution. Analyzing the sources of VOCs revealed that VOCs were found to be affected
484 by a combination of local emissions and regional transport. The primary sources of
485 atmospheric VOCs in Zhengzhou were identified as industrial emissions (32%), vehicle
486 emissions (27%), and combustion (21%). Significant discrepancies were observed in
487 the sources of VOCs between the two pollution processes. In Case 1, industrial
488 emissions constituted the primary source of VOCs, accounting for 32% of the total
489 VOC concentration. In contrast, in Case 2, the proportion of vehicle emissions
490 increased to 33%, representing the primary source of VOCs.

491 A further analysis of the effect of VOCs on SOA generation reveals that aromatic
492 compounds are the primary contributors to SOAP, with BTEX being the predominant
493 contributor throughout the period. The SOAP values reached 37.6 and 65.6 $\mu\text{g}/\text{m}^3$ in
494 Case 1 and Case 2, respectively. In Case 1, the greatest contribution to SOAP was made
495 by industrial sources (63%, 23.8 $\mu\text{g}/\text{m}^3$), while vehicular sources, which constituted the
496 second most important source, accounted for only 18%. In Case 2, the contribution of
497 each VOC source was more evenly distributed, with solvent use sources and fuel

498 evaporation sources representing the primary contributors to SOAP, accounting for 32%
499 (20.9 $\mu\text{g}/\text{m}^3$) and 26% (16.8 $\mu\text{g}/\text{m}^3$), respectively. The SOAP result for the clean day
500 was 8.8 $\mu\text{g}/\text{m}^3$, with industrial sources and solvent use still being the primary
501 contributors. Therefore, the industrial and solvent use sectors are the predominant
502 sources of pollutants during this observation. The aforementioned results substantiate
503 the considerable impact of elevated emissions from all sources on the exacerbation of
504 pollution following the conclusion of the Omicron infection.

505 **Acknowledgments:**

506 This research was supported by the Natural Science Foundation of Henan Province
507 (232300421395) and the National Key Research and Development Program of China
508 (2017YFC0212400).

509 **References**

510 An, J., Zhu, B., Wang, H., Li, Y., Lin, X., and Yang, H.: Characteristics and source
511 apportionment of VOCs measured in an industrial area of Nanjing, Yangtze River Delta,
512 China, *Atmospheric Environment*, 97, 206-214,
513 <https://doi.org/10.1016/j.atmosenv.2014.08.021>, 2014.

514 Bai, L., Lu, X., Yin, S., Zhang, H., Ma, S., Wang, C., Li, Y., and Zhang, R.: A
515 recent emission inventory of multiple air pollutant, PM_{2.5} chemical species and its
516 spatial-temporal characteristics in central China, *Journal of Cleaner Production*, 269,
517 122114, <https://doi.org/10.1016/j.jclepro.2020.122114>, 2020.

518 Buzcu, B. and Fraser, M. P.: Source identification and apportionment of volatile
519 organic compounds in Houston, TX, *Atmospheric Environment*, 40, 2385-2400,
520 <https://doi.org/10.1016/j.atmosenv.2005.12.020>, 2006.

521 Conner, T. L., Lonneman, W. A., Seila, R.L.: Transportation-related volatile
522 hydrocarbon source profiles measured in atlanta, *Journal of the Air & Waste*
523 *Management Association*, 45 (5), 383-394,
524 <https://doi.org/10.1080/10473289.1995.10467370>, 1995.

525 Cui, L., Wu, D., Wang, S., Xu, Q., Hu, R., and Hao, J.: Measurement report:
526 Ambient volatile organic compound (VOC) pollution in urban Beijing: characteristics,
527 sources, and implications for pollution control, *Atmospheric Chemistry and Physics*,
528 22, 11931-11944, <https://doi.org/10.5194/acp-22-11931-2022>, 2022.

529 Derwent, R. G., Jenkin, M. E., Utembe, S. R., Shallcross, D. E., Murrells, T. P.,

530 and Passant, N. R.: Secondary organic aerosol formation from a large number of
531 reactive man-made organic compounds, *Science of the Total Environment*, 408, 3374-
532 3381, <https://doi.org/10.1016/j.scitotenv.2010.04.013>, 2010.

533 Duan, S., Jiang, N., Yang, L., Zhang, R.: *Transport Pathways and Potential Sources*
534 *of PM_{2.5} During the Winter in Zhengzhou*, *Environmental Science*, Jan 8;40(1):86-93,
535 <https://doi.org/10.13227/j.hjcx.201805187>, 2019.

536 Gao, J., Zhang, J., Li, H., Li, L., Xu, L., Zhang, Y., Wang, Z., Wang, X., Zhang,
537 W., Chen, Y., Cheng, X., Zhang, H., Peng, L., Chai, F., and Wei, Y.: Comparative study
538 of volatile organic compounds in ambient air using observed mixing ratios and initial
539 mixing ratios taking chemical loss into account – A case study in a typical urban area
540 in Beijing, *Science of the Total Environment*, 628-629, 791-804,
541 <https://doi.org/10.1016/j.scitotenv.2018.01.175>, 2018.

542 Guan, Y., Liu, X., Zheng, Z., Dai, Y., Du, G., Han, J., Hou, L. a., and Duan, E.:
543 Summer O₃ pollution cycle characteristics and VOCs sources in a central city of
544 Beijing-Tianjin-Hebei area, China, *Environmental Pollution*, 323, 121293,
545 <https://doi.org/10.1016/j.envpol.2023.121293>, 2023.

546 Huang, R., Zhang, Y., Bozzetti, C. et al.: High secondary aerosol contribution to p
547 articulate pollution during haze events in China, *Nature*, 514 (7521), 218–22, <https://doi.org/10.1038/nature13774>, 2014.

549 Hui, L., Liu, X., Tan, Q., Feng, M., An, J., Qu, Y., Zhang, Y., Deng, Y., Zhai, R., a
550 nd Wang, Z.: VOC characteristics, chemical reactivity and sources in urban Wuhan, ce
551 ntral China, *Atmospheric Environment*, 224, 117340, <https://doi.org/10.1016/j.atmosenv.2020.117340>, 2020.

553 Jensen, A., Liu, Z., Tan, W., Dix, B., Chen, T., Koss, A., Zhu, L., Li, L., de Gouw,
554 J.: Measurements of volatile organic compounds during the COVID-19 lockdown in
555 Changzhou, China, *Geophysical research letters*, 48(20), [https://doi.org/10.1029/2021](https://doi.org/10.1029/2021GL095560)
556 [GL095560](https://doi.org/10.1029/2021GL095560), 2021.

557 Jiang, N., Hao, X., Hao, Q., Wei, Y., Zhang, Y., Lyu, Z., Zhang, R.: Changes in se
558 condary inorganic ions in PM_{2.5} at different pollution stages before and after COVID-1
559 9 control, *Environmental Science*, 44(5), 2430-2440, [https://doi.org/10.13227/j.hjcx.2](https://doi.org/10.13227/j.hjcx.202206170)
560 [02206170](https://doi.org/10.13227/j.hjcx.202206170), 2023.

561 Kumar, A., Singh, D., Kumar, K., Singh, B. B., and Jain, V. K.: Distribution of
562 VOCs in urban and rural atmospheres of subtropical India: Temporal variation, source
563 attribution, ratios, OFP and risk assessment, *Science of the Total Environment*, 613-614,

564 492-501, <https://doi.org/10.1016/j.scitotenv.2017.09.096>, 2018.

565 Lai, M., Zhang, D., Yin, S., Song, X., and Zhang, R.: Pollution characteristics,
566 source apportionment and activity analysis of atmospheric VOCs during winter and
567 summer pollution in Zhengzhou City, *Environmental Science*, 4108, 3500-3510,
568 <https://doi.org/10.13227/j.hjkx.202001133>, 2024.

569 Li, B., Ho, S. S. H., Gong, S., Ni, J., Li, H., Han, L., Yang, Y., Qi, Y., and Zhao,
570 D.: Characterization of VOCs and their related atmospheric processes in a central
571 Chinese city during severe ozone pollution periods, *Atmospheric Chemistry and*
572 *Physics*, 19, 617-638, <https://doi.org/10.5194/acp-19-617-2019>, 2019.

573 Li, J., Deng, S., Tohti, A., Li, G., Yi, X., Lu, Z., Liu, J., and Zhang, S.: Spatial
574 characteristics of VOCs and their ozone and secondary organic aerosol formation
575 potentials in autumn and winter in the Guanzhong Plain, China, *Environmental*
576 *Research*, 211, 113036, <https://doi.org/10.1016/j.envres.2022.113036>, 2022.

577 Li, J., Xie, S. D., Zeng, L. M., Li, L. Y., Li, Y. Q., and Wu, R. R.: Characterization
578 of ambient volatile organic compounds and their sources in Beijing, before, during, and
579 after Asia-Pacific Economic Cooperation China 2014, *Atmospheric Chemistry and*
580 *Physics*, 15, 7945-7959, <https://doi.org/10.5194/acp-15-7945-2015>, 2015.

581 Li, J., Lu, K., Lv, W., Li, J., Zhong, L., Ou, Y., Chen, D., Huang, X., and Zhang,
582 Y.: Fast increasing of surface ozone concentrations in Pearl River Delta characterized
583 by a regional air quality monitoring network during 2006–2011, *Journal of*
584 *Environmental Sciences*, 26, 23-36, [https://doi.org/10.1016/S1001-0742\(13\)60377-0](https://doi.org/10.1016/S1001-0742(13)60377-0),
585 2014.

586 Liu, Y., Li, X., Tang, G., Wang, L., Lv, B., Guo, X., and Wang, Y.: Secondary
587 organic aerosols in Jinan, an urban site in North China: Significant anthropogenic
588 contributions to heavy pollution, *Journal of Environmental Sciences*, 80, 107-115,
589 <https://doi.org/10.1016/j.jes.2018.11.009>, 2019.

590 Liu, Y., Shao, M., Fu, L., Lu, S., Zeng, L., and Tang, D.: Source profiles of volatile
591 organic compounds (VOCs) measured in China: Part I, *Atmospheric Environment*, 42,
592 6247-6260, <https://doi.org/10.1016/j.atmosenv.2008.01.070>, 2008.

593 Liu, Y., Song, M., Liu, X., Zhang, Y., Hui, L., Kong, L., Zhang, Y., Zhang, C., Qu,
594 Y., An, J., Ma, D., Tan, Q., and Feng, M.: Characterization and sources of volatile
595 organic compounds (VOCs) and their related changes during ozone pollution days in
596 2016 in Beijing, China, *Environmental Pollution*, 257, 113599,
597 <https://doi.org/10.1016/j.envpol.2019.113599>, 2020.

598 Liu, Z., Hu, K., Zhang, K., Zhu, S., Wang, M., and Li, L.: VOCs sources and roles
599 in O₃ formation in the central Yangtze River Delta region of China, *Atmospheric*
600 *Environment*, 302, <https://doi.org/10.1016/j.atmosenv.2023.119755>, 2023.

601 Li, X., Wang, S., Hao, J.: Characteristics of volatile organic compounds (VOCs)
602 emitted from biofuel combustion in China, *Environmental Science*, 32, 3515-3521,
603 2011.

604 Li, Y., Yin, S., Zhang R., Yu, S., Yang, J., and Zhang, D.: Characteristics and source
605 apportionment of atmospheric VOCs at different pollution levels in winter in an urban
606 area in Zhengzhou, *Environmental Science*, 4108, 3500-3510,
607 <https://doi.org/10.13227/j.hjhx.202001133>, 2020.

608 Ma, Q., Wang, W., Wu, Y., Wang, F., Jin, L., Song, Y., Han, Y., Zhang, R., Zhang,
609 D.: Haze caused by NO_x oxidation under restricted residential and industrial activities
610 in a mega city in the south of North China Plain, *Chemosphere*, Volume 305, 135489,
611 <https://doi.org/10.1016/j.chemosphere.2022.135489>, 2022.

612 Merino, M., Marinescu, M., Cascajo, A., Carretero, J., Singh, D.: Evaluating the
613 spread of Omicron COVID-19 variant in Spain, *Future Generation Computer Systems*,
614 149, 547-561, <https://doi.org/10.1016/j.future.2023.07.025>, 2023.

615 Monod, A., Sive, B. C., Avino, P., Chen, T., Blake, D. R., and Sherwood Rowland,
616 F.: Monoaromatic compounds in ambient air of various cities: a focus on correlations
617 between the xylenes and ethylbenzene, *Atmospheric Environment*, 35, 135-149,
618 [https://doi.org/10.1016/S1352-2310\(00\)00274-0](https://doi.org/10.1016/S1352-2310(00)00274-0), 2001.

619 Mozaffar, A., Zhang, Y.-L., Fan, M., Cao, F., and Lin, Y.-C.: Characteristics of
620 summertime ambient VOCs and their contributions to O₃ and SOA formation in a
621 suburban area of Nanjing, China, *Atmospheric Research*, 240, 104923,
622 <https://doi.org/10.1016/j.atmosres.2020.104923>, 2020.

623 Mu, L., Feng, C., Li, Y., Li, X., Liu, T., Jiang, X., Liu, Z., Bai, H., and Liu, X.:
624 Emission factors and source profiles of VOCs emitted from coke production in Shanxi,
625 China, *Environmental Pollution*, 335, 122373,
626 <https://doi.org/10.1016/j.envpol.2023.122373>, 2023.

627 Niu, Y., Yan, Y., Chai, J., Zhang, X., Xu, Y., Duan, X., Wu, J., and Peng, L.: Effects
628 of regional transport from different potential pollution areas on volatile organic
629 compounds (VOCs) in Northern Beijing during non-heating and heating periods,
630 *Science of the Total Environment*, 836, 155465,
631 <https://doi.org/10.1016/j.scitotenv.2022.155465>, 2022.

632 Norris, G., Duvall, R., Brown, S., Bai, S. EPA Positive Matrix Factorization (PMF)
633 5.0 Fundamentals and User Guide. U.S. Environmental Protection Agency, Washington,
634 DC, EPA/600/R-14/108 (NTIS PB2015-105147), 2014.

635 Paatero, P., Eberly, S., Brown, S. G., Norris, G. A.: Methods for estimating
636 uncertainty in factor analytic solutions, *Atmospheric Measurement Techniques*, Volume
637 7, 781-797, <https://doi.org/10.5194/amt-7-781-2014>, 2014.

638 Pei, C., Yang, W., Zhang, Y., Song, W., Xiao, S., Wang, J., Zhang, J., Zhang, T.,
639 Chen, D., Wang, Y., Chen, Y., Wang, X.: Decrease in ambient volatile organic
640 compounds during the COVID-19 lockdown period in the Pearl River Delta region,
641 south China, *Science of The Total Environment*, 823, 153720,
642 <https://doi.org/10.1016/j.scitotenv.2022.153720>, 2022.

643 Petersen, M. S., Í Kongsstovu, S., Eliassen, E. H., Larsen, S., Hansen, J. L., Vest,
644 N., Dahl, M. M., Christiansen, D. H., Møller, L. F., & Kristiansen, M. F.: Clinical
645 characteristics of the Omicron variant - results from a Nationwide Symptoms Survey
646 in the Faroe Islands, *International Journal of Infectious Diseases*, 122, 636–643,
647 <https://doi.org/10.1016/j.ijid.2022.07.005>, 2022.

648 Qi, J., Mo, Z., Yuan, B., Huang, S., Huangfu, Y., Wang, Z., Li, X., Yang, S., Wang,
649 W., Zhao, Y., Wang, X., Wang, W., Liu, K., and Shao, M.: An observation approach in
650 evaluation of ozone production to precursor changes during the COVID-19 lockdown,
651 *Atmospheric Environment*, 262, 118618,
652 <https://doi.org/10.1016/j.atmosenv.2021.118618>, 2021.

653 Russo, R. S., Zhou, Y., White, M. L., Mao, H., Talbot, R., and Sive, B. C.: Multi-
654 year (2004–2008) record of nonmethane hydrocarbons and halocarbons in New
655 England: seasonal variations and regional sources, *Atmospheric Chemistry and Physics*,
656 10, 4909-4929, <https://doi.org/10.5194/acp-10-4909-2010>, 2010.

657 Sahu, L. K., Tripathi, N., Gupta, M., Singh, V., Yadav, R., Patel, K.: Impact of
658 COVID-19 Pandemic lockdown in ambient concentrations of aromatic volatile organic
659 compounds in a metropolitan city of western India, *Journal of geophysical research*,
660 *Atmospheres : JGR*, 127(6), <https://doi.org/10.1029/2022JD036628>, 2022.

661 Schauer, J., Kleeman, M., Cass, G., Simoneit, B.: Measurement of emissions from
662 air pollution sources.5. C₁-C₃₂ organic compounds from gasoline-powered motor
663 vehicles, *Environmental Science & Technology*, 36, 1169-1180,
664 <https://doi.org/10.1021/es0108077>, 2002.

665 Shao, P., An, J., Xin, J., Wu, F., Wang, J., Ji, D., and Wang, Y.: Source

666 apportionment of VOCs and the contribution to photochemical ozone formation during
667 summer in the typical industrial area in the Yangtze River Delta, China, *Atmospheric*
668 *Research*, 176-177, 64-74, <https://doi.org/10.1016/j.atmosres.2016.02.015>, 2016.

669 Shi, Y., Liu, C., Zhang, B., Simayi, M., Xi, Z., Ren, J., and Xie, S.: Accurate
670 identification of key VOCs sources contributing to O₃ formation along the Liaodong
671 Bay based on emission inventories and ambient observations, *Science of the Total*
672 *Environment*, 844, 156998, [10.1016/j.scitotenv.2022.156998](https://doi.org/10.1016/j.scitotenv.2022.156998), 2022.

673 Singh, B., Sohrab, S., Athar, M., Alandijany, T., Kumari, S., Nair, A., Kumari, S.,
674 Mehra, K., Chowdhary, K., Rahman, S., Azhar, E.: Substantial changes in selected
675 volatile organic compounds (VOCs) and associations with health risk assessments in
676 industrial areas during the COVID-19 Pandemic, *Toxics*, 11, 165,
677 <https://doi.org/10.3390/toxics11020165>, 2023a.

678 Singh, B., Singh, M., Ulman, Y., Sharma, U., Pradhan, R., Sahoo, J., Padhi, S.,
679 Chandra, P., Koul, M., Tripathi, P., Kumar, D., Masih, J.: Distribution and temporal
680 variation of total volatile organic compounds concentrations associated with health risk
681 in Punjab, India, *Case Studies in Chemical and Environmental Engineering*, 8, 100417,
682 <https://doi.org/10.1016/j.cscee.2023.100417>, 2023b.

683 Song, M., Li, X., Yang, S., Yu, X., Zhou, S., Yang, Y., Chen, S., Dong, H., Liao,
684 K., Chen, Q., Lu, K., Zhang, N., Cao, J., Zeng, L., and Zhang, Y.: Spatiotemporal
685 variation, sources, and secondary transformation potential of volatile organic
686 compounds in Xi'an, China, *Atmospheric Chemistry and Physics*, 21, 4939-4958,
687 <https://doi.org/10.5194/acp-21-4939-2021>, 2021.

688 Song, X., Zhang, D., Li, X., Lu, X., Wang, M., Zhang, B., Zhang, R.: Simultaneous
689 observations of peroxyacetyl nitrate and ozone in Central China during static
690 management of COVID-19: Regional transport and thermal decomposition,
691 *Atmospheric Research*, Volume 294, 106958,
692 <https://doi.org/10.1016/j.atmosres.2023.106958>, 2023.

693 Song, Y., Shao, M., Liu, Y., Lu, S., Kuster, W., Goldan, P., and Xie, S.: Source
694 apportionment of ambient volatile organic compounds in Beijing, *Environmental*
695 *Science & Technology*, 41, 4348-4353, <https://doi.org/10.1021/es0625982>, 2007.

696 Wang, H., Li, J., Peng, Y., Zhang, M., Che, H., Zhang, X.: The impacts of the
697 meteorology features on PM_{2.5} levels during a severe haze episode in central-east
698 China, *Atmospheric Environment*, Volume 197, Pages 177-189, ISSN 1352-2310,
699 <https://doi.org/10.1016/j.atmosenv.2018.10.001>, 2019.

700 Wang, H., Wang, Q., Chen, J. Chen, C., Huang, C., Qiao, L. Lou, S., Lu, J.: Do
701 vehicular emissions dominate the source of C6–C8 aromatics in the megacity Shanghai
702 of eastern China?, *Environmental Science*, 27, 290-297, [https://doi.org/10.](https://doi.org/10.1016/j.jes.2014.05.033)
703 1016/j.jes.2014.05.033, 2015.

704 Wang, M., Lu, S., Shao, M., Zeng, L., Zheng, J., Xie, F., Lin, H., Hu, K., and Lu,
705 X.: Impact of COVID-19 lockdown on ambient levels and sources of volatile organic
706 compounds (VOCs) in Nanjing, China, *Science of the Total Environment*, 757, 143823,
707 <https://doi.org/10.1016/j.scitotenv.2020.143823>, 2021.

708 Wang, M., Zeng, L., Lu, S., Shao, M., Liu, X., Yu, X., Chen, W., Yuan, B., Zhang,
709 Q., Hu, M., & Zhang, Z.: Development and validation of a cryogen-free automatic gas
710 chromatograph system (GC-MS/FID) for online measurements of volatile organic
711 compounds, *Analytical Methods*, 6, 9424, <https://doi.org/10.1039/C4AY01855A>, 2014.

712 Wang, T., Xue, L., Brimblecombe, P., Lam, Y. F., Li, L., and Zhang, L.: Ozone
713 pollution in China: A review of concentrations, meteorological influences, chemical
714 precursors, and effects, *Science of the Total Environment*, 575, 1582-1596,
715 <https://doi.org/10.1016/j.scitotenv.2016.10.081>, 2017.

716 Wu, R., Li, J., Hao, Y., Li, Y., Zeng, L., and Xie, S.: Evolution process and sources
717 of ambient volatile organic compounds during a severe haze event in Beijing, China,
718 *Science of the Total Environment*, 560-561, 62-72,
719 <https://doi.org/10.1016/j.scitotenv.2016.04.030>, 2016.

720 Wu, W., Zhao, B., Wang, S., and Hao, J.: Ozone and secondary organic aerosol
721 formation potential from anthropogenic volatile organic compounds emissions in China,
722 *Journal of Environmental Sciences*, 53, 224-237,
723 <https://doi.org/10.1016/j.jes.2016.03.025>, 2017.

724 Xiong, Y., Zhou, J., Xing, Z., and Du, K.: Optimization of a volatile organic
725 compound control strategy in an oil industry center in Canada by evaluating ozone and
726 secondary organic aerosol formation potential, *Environmental Research*, 191, 110217,
727 <https://doi.org/10.1016/j.envres.2020.110217>, 2020.

728 Yun, L., Li, C., Zhang, M., He, L. and Guo, J.: Pollution characteristics and sources
729 of atmospheric VOCs in the coastal background area of the Pearl River Delta,
730 *Environmental Science*, 4191-4201, <https://doi.org/10.13227/j.hjcx.202101155>, 2021.

731 Zeng, X., Han, M., Ren, G., Liu, G., Wang, X., Du, K., Zhang, X., and Lin, H.: A
732 comprehensive investigation on source apportionment and multi-directional regional
733 transport of volatile organic compounds and ozone in urban Zhengzhou, *Chemosphere*,

734 334, 139001, <https://doi.org/10.1016/j.chemosphere.2023.139001>, 2023.

735 Zhang, C., Liu, X., Zhang, Y., Tan, Q., Feng, M., Qu, Y., An, J., Deng, Y., Zhai, R.,
736 Wang, Z., Cheng, N., and Zha, S.: Characteristics, source apportionment and chemical
737 conversions of VOCs based on a comprehensive summer observation experiment in
738 Beijing, *Atmospheric Pollution Research*, 12, 230-241,
739 <https://doi.org/10.1016/j.apr.2020.12.010>, 2021a.

740 Zhang, D., He, B., Yuan, M., Yu, S., Yin, S., and Zhang, R.: Characteristics,
741 sources and health risks assessment of VOCs in Zhengzhou, China during haze
742 pollution season, *Journal of Environmental Sciences*, 108, 44-57,
743 <https://doi.org/10.1016/j.jes.2021.01.035>, 2021b.

744 Zhang, D., Li, X., Yuan, M., Xu, Y., Xu, Q., Su, F., Wang, S., Zhang, R.:
745 Characteristics and sources of nonmethane volatile organic compounds (NMVOCs) and
746 O₃-NO_x-NMVOC relationships in Zhengzhou, China, *Atmosphere Chemistry and
747 Physics*, 24, 8549-8567, <https://doi.org/10.5194/acp-24-8549-2024>, 2024.

748 Zhang, F., Shang, X., Chen, H., Xie, G., Fu, Y., Wu, D., Sun, W., Liu, P., Zhang,
749 C., Mu, Y., Zeng, L., Wan, M., Wang, Y., Xiao, H., Wang, G., and Chen, J.: Significant
750 impact of coal combustion on VOCs emissions in winter in a North China rural site,
751 *Science of the Total Environment*, 720, 137617,
752 <https://doi.org/10.1016/j.scitotenv.2020.137617>, 2020.

753 Zhang, J., Sun, Y., Wu, F., Sun, J., and Wang, Y.: The characteristics, seasonal
754 variation and source apportionment of VOCs at Gongga Mountain, China, *Atmospheric
755 Environment*, 88, 297-305, <https://doi.org/10.1016/j.atmosenv.2013.03.036>, 2014.

756 Zhang, Z., Yan, X., Gao, F., Thai, P., Wang, H., Chen, D., Zhou, L., Gong, D., Li,
757 Q., Morawska, L., and Wang, B.: Emission and health risk assessment of volatile
758 organic compounds in various processes of a petroleum refinery in the Pearl River Delta,
759 China, *Environmental Pollution*, 238, 452-461,
760 <https://doi.org/10.1016/j.envpol.2018.03.054>, 2018.

761 Zheng, H., Kong, S., Xing, X., Mao, Y., Hu, T., Ding, Y., Li, G., Liu, D., Li, S.,
762 and Qi, S.: Monitoring of volatile organic compounds (VOCs) from an oil and gas
763 station in northwest China for 1 year, *Atmospheric Chemistry and Physics*, 18, 4567-
764 4595, <https://doi.org/10.5194/acp-18-4567-2018>, 2018.

765 Zheng, J., Zhong, L., Wang, T., Louie, P. K. K., and Li, Z.: Ground-level ozone in
766 the Pearl River Delta region: Analysis of data from a recently established regional air
767 quality monitoring network, *Atmospheric Environment*, 44, 814-823,

768 <https://doi.org/10.1016/j.atmosenv.2009.11.032>, 2010.

769 Zhou, Z., Xiao, L., Fei, L., Yu, W., Lin M., Huang, T., Zhang, Z. and Tao J.:
770 Characteristics and sources of VOCs during ozone pollution and non-pollution periods
771 in summer in Dongguan industrial concentration area, *Environmental Science*, 4497-
772 4505, <https://doi.org/10.13227/j.hjkx.202111285>, 2022.

773 Zou, Y., Yan, X. L., Flores, R. M., Zhang, L. Y., Yang, S. P., Fan, L. Y., Deng, T.,
774 Deng, X. J., and Ye, D. Q.: Source apportionment and ozone formation mechanism of
775 VOCs considering photochemical loss in Guangzhou, China, *Science of the Total*
776 *Environment*, 903, 166191, <https://doi.org/10.1016/j.scitotenv.2023.166191>, 2023.

777 Zuo, H., Jiang, Y., Yuan, J., Wang, Z., Zhang, P., Guo, C., Wang, Z., Chen, Y., Wen,
778 Q., Wei, Y., Li, X.: Pollution characteristics and source differences of VOCs before and
779 after COVID-19 in Beijing, *Science of The Total Environment*, 907, 167694,
780 <https://doi.org/10.1016/j.scitotenv.2023.167694>, 2024.

781